Rare Metal Materials and Engineering
Volume 46, Issue 3, March 2017
Online English edition of the Chinese language journal

Available online at www.sciencedirect.com
ScienceDirect

Cite this article as: Rare Metal Materials and Engineering, 2017, 46(3): 0612-0616.

ARTICLE

Effects of Laser Cladding Layers Width on Total Indicated Runout Characteristics of Steam Turbine Rotor Surface

Guo Shirui[1], Shang Huichao[1], Cui Lujun[1], Guo Xiaofeng[1], Yao Jianhua[2,3]

[1] Zhongyuan University of Technology, Zhengzhou 450007, China; [2] Zhejiang University of Technology, Hangzhou 310014, China; [3] Zhejiang Provincial Collaborative Innovation Center of High-end Laser Manufacturing Equipment, Hangzhou 310014, China

Abstract: In order to solve the wear repair problem of large steam turbine rotor shaft journal, the material of steam turbine rotor shaft was used as a substrate and the self-made special laser cladding remanufacturing powder as the experimental material, and the experiments were carried out by a laser cladding remanufacturing method based on the laser cladding remanufacturing system with coaxial powder feeder. Focusing on effect of different widths of laser cladding layers on total indicated runout (TIR) of steam turbine rotor, the experiment research and mechanism simulation verification were performed, and the influence mechanism of different factors were analyzed. The total data indicates runout are closely related to probe diameter and laser cladding layer width. The width of cladding layer determines the turbine rotor surface magnetic, eddy current density and magnetic flux density distribution. Due to the interference of matrix magnetic field and eddy current density of the surface, the magnetic flux density suddenly changes in the laser cladding layer edge when the laser cladding layer width is less than 8 mm. The measurement results are too large caused by the comprehensive effect of the substrate and the laser cladding layer. According to the numerical simulation of magnetic flux density distribution of measured metal body surface, the critical value of laser cladding width is 9.82 mm.

Key words: laser cladding; total indicated runout; eddy current sensor; numerical simulation; steam turbine rotor

Laser cladding green remanufacturing is a new advanced technology. Compared with other traditional techniques, it has many advantages, such as short acting time, low dilution rate of repair layer, small heat affected zone in the repair area, small deformation of the workpiece, fast cooling speed, refinement, grain metastable phase, the amorphous phase and the super dispersion[1,2]. It can not only restore the shape size of damaged parts, but also make the performance of damaged parts reach even beyond the level of new products. Large steam turbine rotor shaft neck is easy to wear. Because of its large size, high weight, high accuracy, complex production process, high production cost, long processing cycle, it will make a tremendous impact once the problem occurs in operation[3,4]. If the local damage of the turbine rotor is repaired befor reused, it will save a lot of production cost. Tabernero and Richter[5,6] studied the laser repairing of turbine rotors and blades and found that the performance of the laser cladding was superior to that of the substrate material, and proposed that laser cladding technique was promising to repair turbine components.

At present, the research of laser cladding steam turbine rotor is generally only related to microstructure of cladding layer. One of the major concerns for laser repaired rotors of steam turbine units is total indicated runout (TIR), which is the synergetic effect of mechanical runout and electrical runout[7]. Mechanical runout is mainly a measure of the non-roundness of rotor shaft using a micrometer gauge and electrical runout is mainly a measure of the change of electromagnetic properties on the shaft[8]. The sum of these two types of runout, is termed total indicated runout. According to American Petroleum Institute (API) No.612 standards for compressors and turbines, the total indicated runout value for the components of these units should be

Received date: March 25, 2016
Foundation item: Key Scientific Research Project for Colleges and Universities of Henan Province (15A460038); National Natural Science Foundation of China (51505506)
Corresponding author: Guo Shirui, Ph. D., Lecturer, Zhongyuan University of Technology, Zhengzhou 450007, P. R. China, Tel: 0086-371-62506077, E-mail: laser@zut.edu.cn

controlled within 6.35 μm, and the products exceeding this value will be scrapped or reworked[9]. The existing researches are seldom to discuss the total indicated runout characteristics of steam turbine. In the present research, the laser cladding repair of a large rotary component was studied by the high power diode laser. The different laser cladding layers of steam turbine rotor surface were tested for total indicated runout, and the mechanism was analyzed by Ansys software. The cladded shaft with the lowest runout was considered to have the best performance in service. The outcome of this research provided the steam turbine industry with useful information on large rotary component reparations.

1 Experiment

Steam turbine rotor belongs to whole forging type rotor according to the combination between the main shaft and other components. Laser alloy powders were deposited on a rotor shaft by a laser cladding process. The shaft was a 28CrMoNiV stainless steel cylinder with the diameter of 125.50 mm. The particle size of laser cladding alloy powder was 45~109 m. The chemical composition of shaft and laser cladding alloy powder is shown in Table 1.

Laser cladding experiment was performed using high power flexible fiber-coupled diode laser with a type of LDF400-2000. The output wavelength was 900 ~ 1030 nm and the maximum output power was 2000 W. A circular spot was adopted in the cladding process with two fixed spot sizes of 2 mm, and argon gas protective laser pool. The cladding system had a self-generating coaxial powder feeding device and closed loop feedback, and the feeding range was 2~50 g/min. Argon was used as carrier and support gas. The motion device for powder feeding was IRB2400/16 robot with 6 degrees of freedom. The main processing parameters of laser cladding are listed in Table 2.

The measurement of total indicated runout value was carried out by eddy current sensor with laser cladding coating step by step grinding. During the testing process, the speed of the rotor shaft was 30r/min, and the test procedure is shown in Fig.1.

In the investigation of effect of different laser cladding layer widths on induced magnetic field and eddy current distribution, because shaft section was measured in case of 30 r/m in the actual total indicated runout testing process, the main view local amplification of the cross section can be seen as a transient equilibrium[9]. In addition, the measurement process was an axial symmetry, the model can be simplified, the half coil was regarded as a rectangular, and the laser cladding layer thickness was 0.5 mm, as shown in Fig.2. Thus the 3D model was simplified as a two-dimensional axisymmetric mode. The problem of three dimensional eddy current field was simplified as an axisymmetric quasi stationary electromagnetic field. By changing laser cladding layer width L, the influence of magnetic field and eddy current distribution can be researched.

In the Ansys analysis, flux parallel boundary conditions (the magnetic potential 0) were only considered in the periphery of the plane region. That was the first class boundary condition.

Table 1 Chemical composition of alloy powder F1 and 28CrMoNiV (wt%)

Material	C	Cr	Si	Mo	Mn	Fe	Ni	V
Laser cladding alloy powder	0.25~0.3	3.0~5.0	≤1.00	0.5~0.9	≤3.00	Bal.	–	–
28CrMoNiV	0.25~0.3	1.1~1.4	≤0.30	0.8~1	0.3~0.8	Bal.	0.5~0.75	0.25~0.35

Table 2 Process parameters of laser cladding

D/mm	P/W	V_s/mm·min^{-1}	V_f/g·min^{-1}	η/%
4	1800	440	10	40

Note: D-laser spot diameter, P-laser power, V_s-rotational speed of shaft, V_f -powder feeding speed, η-overlap rate

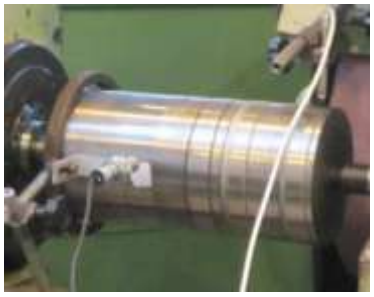

Fig.1 Testing of total indicated runout

Further in the analysis, the input voltage, coupling current, voltage degree of freedom and other constraints condition needed to be applied. The physical performance parameters of the probe coil and the shaft section material at room temperature came from the access to information. The 28CrMoNiV parameter was unknown, so the parameters of 35Cr2Ni4Mo with similar chemical composition were used. The simulation data is shown in Table 3.

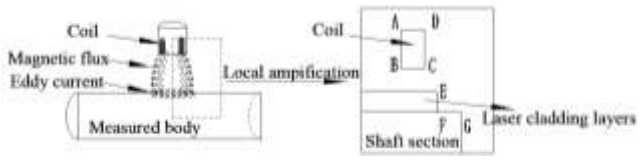

Fig.2 Computational geometry model for the influence of alloy materials on electromagnetic field

Table 3 Simulation data used in this study

Item	Value
Outside diameter of probe coil/mm	7
Inner diameter of probe coil/mm	5
Height of probe coil/mm	2
Area of single probe coil/(mm×mm)	2
Total number of probe coil	139
Wire diameter of each probe coil/mm	0.12
Detection distance/mm	1.2
Relative permeability of probe coil	0.99999
Resistivity of probe coil/Ω·m	1.7×10^{-8}
Detection frequency/Hz	10^6
Excitation voltage/V	24
Relative permeability of measured shaft section	4000
Resistivity of measured shaft section/Ω·m	4.4×10^{-7}

2 Results and Discussion

2.1 Analysis of the results of total indicated runout test

Fig.3 presents the morphology of the turbine rotor shaft section after laser cladding, and the material of laser cladding layer is F1 iron-based alloy. The coating widths from left to right are 8, 16, 24 and 32 mm. After the experiment, the same measurement method was used to measure the total indicated runout value of four kinds of the cladding layer. The total indicated runout results are shown in Fig.4. After measuring, when the laser cladding layers width is 8 mm, the total indicated runout value is more than that of other laser cladding layers width.

As it can be seen from Fig.5, different coil radii of eddy current sensor probe generated magnetic field range are different. When the magnetic field generated by the probe coil is certain, the eddy current field formed on the surface of the measured body is also certain. As a result, the width L of detection range is certain when the probe coil in a fixed detection distance of x, and the specific range varies with the radius of the probe coil. Supposing the measured metal body surface is flat, Fig.6 can be obtained by simplifying schematic diagram of eddy current distribution range in Fig.5.

When the measured surface of the metal body is flat, the geometry size of eddy current region can be calculated according to the empirical formula: c=0.86r, r_i=0.53r_b, r_a=1.39r_b. Coil winding thickness is 1 mm, internal coil height

Fig.3 Morphology of shaft section by laser cladding

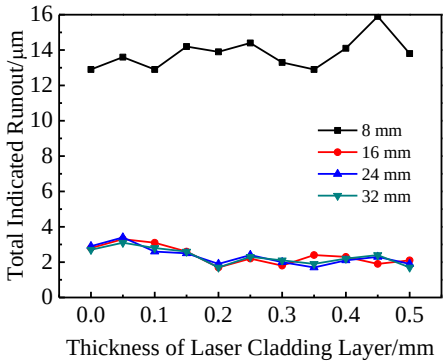

Fig.4 Measurement data of total indicated runout

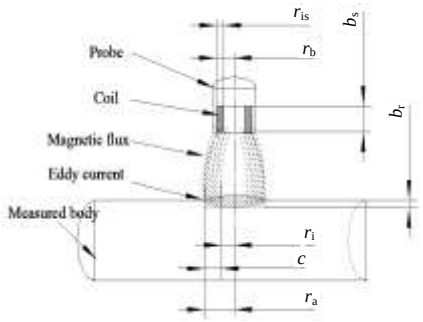

b_s: the height of internal coil of the eddy current sensor probe; r_{is}: coil winding thickness; r_b: the distance from the outer diameter of the coil to the centerline of the eddy current sensor probe; b_r: the penetration depth of eddy current of measured body; c: the width of eddy current effect; r_a: the distance between the external diameter of eddy current effect and the centerline of the eddy current sensor probe; in theory, the region of r_i whose width is r_a-c is no eddy current

Fig.5 Schematic diagram of eddy current distribution

of the modified Bentley eddy current sensor (8 mm 3300XL) probe is 2 mm in the experiment. The distance between the external diameter of eddy current effect and the centerline of the eddy current sensor probe is 3.5 mm. Through the above data can be obtained the width of eddy current effect is 3.01 mm, the distance between the external diameter of eddy current effect and the centerline of the eddy current sensor probe is 4.865 mm and the width of r_i is 1.855 mm.

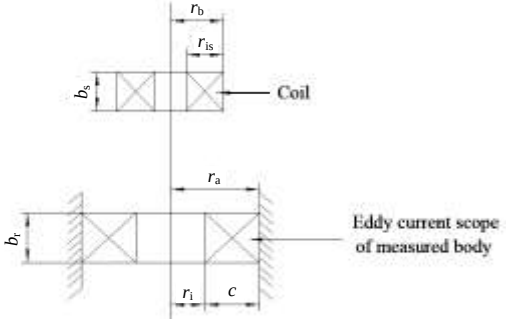

Fig.6 Simplified diagram of eddy current distribution

2.2 Distribution of magnetic line of force

Effect of laser cladding layer width 8, 16, 24 and 32 mm on magnetic line of force distribution characteristics was simulated under the same shaft section materials, the same laser cladding layer material and other same conditions, as shown in Fig.7.

With the gradual increase of laser cladding layer width, the magnetic line of force changes obviously. The periphery of the magnetic induction intensity is weak and the magnetic induction intensity in the center of the ring is the strongest. The right part of two magnetic lines of force are not through the laser cladding layers, but through the shaft section directly, and even a line is not through any measured body in Fig.7a; that is the result of limited measurement width of laser cladding layer. According to the experimental results and Fig.7, the fourth ring magnetic line of force smooth through the laser cladding layers largely determines its total indicated runout measurement value. Fig.7a shows that, when the width of laser cladding layer is 8 mm, the magnetic line of force does not laterally go across the laser cladding layer, but through the vertical shaft section directly; the actual measurement total indicated runout value is the result of the interaction between the substrate material and the laser cladding layers material.

2.3 Distribution of eddy current field

Effect of laser cladding layer width 8, 16, 24 and 32 mm on eddy current field distribution characteristics of measured metal body was simulated under the same conditions, as shown in Fig.8.

The eddy current density in the surface of the laser cladding layer is asymmetric in Fig.8a. The eddy current density of the right edge is the largest, and gradually reduced to the internal. On the binding site between the right side of the laser cladding layer and the shaft section, eddy current density increases suddenly and gradually decrease along the depth direction, and that is significantly different in Fig.8b, Fig.8c and Fig.8d. This shows that the width of the laser cladding layers is too small, and the eddy current of substrate material and laser cladding layers are superimposed influence. The width of the laser cladding layers also determines the flat belt distribution of eddy current field in the measured surface. The flat belt is expressed as the same density of the eddy current distribution.

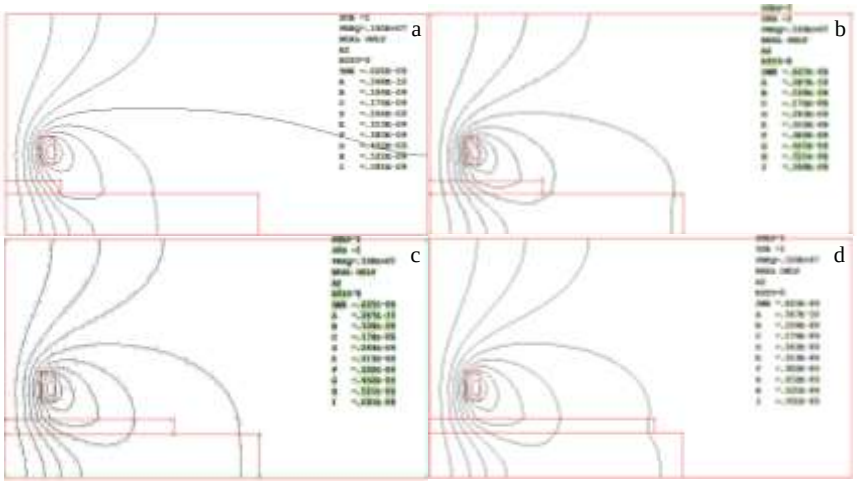

Fig.7 Magnetic line of force distribution of different width of laser cladding layers: (a) 8 mm, (b) 16 mm, (c) 24 mm, and (d) 32 mm

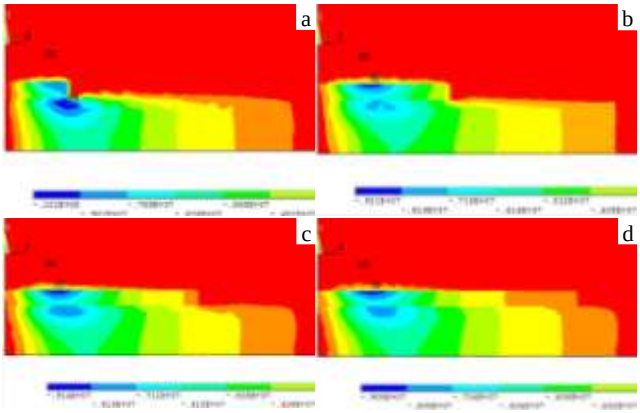

Fig.8 Eddy current field distribution of different widths of laser cladding layers: (a) 8 mm, (b) 16 mm, (c) 24 mm, and (d) 32 mm

Eddy current distribution of the same density can reduce the influence of dissimilar materials and the error of the measurement. When the width of the laser cladding layers is 8 mm, the surface eddy current density of the layer is affected by the substrate material, so the measurement value of total indicated runout is too large in the experiment.

2.4 Distribution of magnetic flux density

When the surface of measured metal body is flat, the effect width of eddy current is $2r_a$, which is 9.73 mm. From the experimental data, the width of the laser remanufacturing layer should exceed a certain value in the 8~16 mm range. Because one side of measured surface is a curved surface and other side is a flat, the effect width of eddy current should be slightly greater than that of flat. The results of empirical formula 9.73 mm only be used as a reference, and can't be used

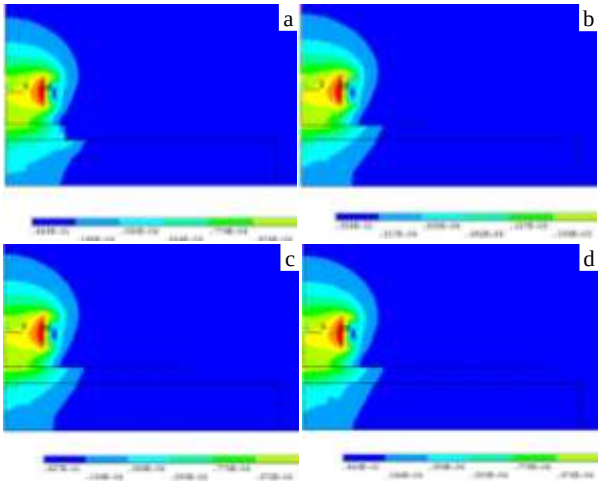

Fig.9 Magnetic flux density distribution of different width of laser cladding layers: (a) 8 mm, (b) 16 mm, (c) 24 mm, and (d) 32 mm

as the conclusion of the critical value of the laser remanufacturing layer width. As it can be seen from Fig.9, with the laser cladding layer width gradual increasing, the magnetic flux density of the electromagnetic field around the probe coil is the same as that of the ambient air portion. Due to the limitation of laser cladding layer width in Fig.9a, the magnetic flux density suddenly changes on the edge of the laser cladding layer. The measurement results are too largely affected by the change of magnetic flux density. In Fig.9b~9d, the magnetic flux density of the laser cladding layers and the substrate is a smooth transition. As the magnetic flux density is the basis of the total indicated runout measurement, it can be calculated that the critical width of the laser cladding layers is 9.82 mm based on Fig.9.

3 Conclusions

1) The results of the total indicated runout data are closely related to the width of the laser cladding layers through the numerical simulation based on experiment verification. When the laser cladding layer is less than 8 mm, due to the magnetic line of force and eddy current density in the surface of the laser cladding layer by substrate interference, the actual measurement results of total indicated runout are the comprehensive effect of substrate and laser cladding layer.

2) Due to the limitation of laser cladding layer width, the magnetic flux density suddenly changes on the edge of the laser cladding layer. The measurement results are too largely affected by the change of magnetic flux density. According to the numerical simulation of magnetic flux density distribution of measured metal body surface, the critical value of laser cladding width is 9.82 mm.

References

1 Li L. *Optics and Lasers in Engineering*[J], 2000, 34(4): 231
2 Xu B S. *Surface Engineering*[J], 2010, 26(1-2): 123
3 Lu Y H, Yuan L J, Cai D B *et al*. *Rare Metal Materials and Engineering*[J], 2014, 43(10): 2349
4 Xu B S, Dong S Y, Zhu S *et al*. *Journal of Mechanical Engineering*[J], 2012, 48(8): 96
5 Tabernero I, Lamikiz A, Martinez S *et al*. *International Journal of Machine Tools & Manufacture*[J], 2011, 51(6): 465
6 Richter K H, Orban S, Nowotny S. *23rd International Conference on Applications of Laser and Electro-Optics*[C]. US: Laser Institute of America, 2004
7 Guo S R, Lai H M, Kong J Q *et al*. *32nd International Conference on Applications of Laser and Electro-Optics*[C]. US: Laser Institute of America, 2013
8 ANSI/API 612-1995[S], 1995
9 Wang Y F, Cao Y L, Chen X L *et al*. *Sensors & Transducers*[J], 2014, 162: 266

激光熔覆层宽度对汽轮机转子表面综合跳动特性的影响

郭士锐[1]，尚会超[1]，崔陆军[1]，郭小锋[1]，姚建华[2,3]
(1. 中原工学院，河南 郑州 450007)
(2. 浙江工业大学，浙江 杭州 310014)
(3. 浙江省高端激光制造装备协同创新中心，浙江 杭州 310014)

摘 要：为解决大型汽轮机转子轴轴颈磨损的修复问题，基于同轴送粉半导体激光熔覆再制造系统，采用激光熔覆再制造方法，以汽轮机转子轴材料为基体，利用激光熔覆再制造专用粉末作为实验材料，针对不同激光熔覆层宽度对汽轮机转子综合跳动的影响进行实验研究与机理模拟验证。结果表明，综合跳动特性与探头直径和激光熔覆层宽度相关，激光熔覆层宽度决定了汽轮机转子表面磁力线、电涡流密度与磁通量密度分布。当激光再制造层宽度小于 8 mm 时，由于磁力线与表面电涡流密度受基体的干扰，磁通量密度在激光熔覆层的边缘出现突变，实际综合跳动的测量值为基体与激光熔覆层综合作用的结果，造成测量结果偏大。根据数值模拟计算被测金属体表面磁通量密度分布结果，激光熔覆层宽度的临界值为 9.82 mm。

关键词：激光熔覆；综合跳动；电涡流传感器；数值模拟；汽轮机转子

作者简介：郭士锐，男，1986 年生，博士，讲师，中原工学院机电学院，河南 郑州 450007，电话：0371-62506077，E-mail: j10312@163.com